

Measurement of the B^- and \bar{B}^0 Meson Lifetimes Using Semileptonic Decays

- F. Abe,¹⁴ H. Akimoto,³² A. Akopian,²⁷ M. G. Albrow,⁷ S. R. Amendolia,²³ D. Amidei,¹⁷ J. Antos,²⁹ C. Anway-Wiese,⁴ S. Aota,³² G. Apollinari,²⁷ T. Asakawa,³² W. Ashmanskas,¹⁵ M. Atac,⁷ F. Azfar,²² P. Azzi-Bacchetta,²¹ N. Bacchetta,²¹ W. Badgett,¹⁷ S. Bagdasarov,²⁷ M. W. Bailey,¹⁹ J. Bao,³⁵ P. de Barbaro,²⁶ A. Barbaro-Galtieri,¹⁵ V. E. Barnes,²⁵ B. A. Barnett,¹³ E. Barzi,⁸ G. Bauer,¹⁶ T. Baumann,⁹ F. Bedeschi,²³ S. Behrends,³ S. Belforte,²³ G. Bellettini,²³ J. Bellinger,³⁴ D. Benjamin,³¹ J. Benloch,¹⁶ J. Bensinger,³ D. Benton,²² A. Beretvas,⁷ J. P. Berge,⁷ J. Berryhill,⁵ S. Bertolucci,⁸ A. Bhatti,²⁷ K. Biery,¹² M. Binkley,⁷ D. Bisello,²¹ R. E. Blair,¹ C. Blocker,³ A. Bodek,²⁶ W. Bokhari,¹⁶ V. Bolognesi,⁷ D. Bortoletto,²⁵ J. Boudreau,²⁴ L. Breccia,² C. Bromberg,¹⁸ N. Bruner,¹⁹ E. Buckley-Geer,⁷ H. S. Budd,²⁶ K. Burkett,¹⁷ G. Busetto,²¹ A. Byon-Wagner,⁷ K. L. Byrum,¹ J. Cammerata,¹³ C. Campagnari,⁷ M. Campbell,¹⁷ A. Caner,⁷ W. Carithers,¹⁵ D. Carlsmith,³⁴ A. Castro,²¹ D. Cauz,²³ Y. Cen,²⁶ F. Cervelli,²³ P. Auchincloss,²⁶ H. Y. Chao,²⁹ J. Chapman,¹⁷ M.-T. Cheng,²⁹ G. Chiarelli,²³ T. Chikamatsu,³² C. N. Chiou,²⁹ L. Christofek,¹¹ S. Cihangir,⁷ A. G. Clark,²³ M. Cobal,²³ M. Contreras,⁵ J. Conway,²⁸ J. Cooper,⁷ M. Cordelli,⁸ C. Couyoumtzelis,²³ D. Crane,¹ D. Cronin-Hennessy,⁶ R. Culbertson,⁵ J. D. Cunningham,³ T. Daniels,¹⁶ F. DeJongh,⁷ S. Delchamps,⁷ S. Dell'Agnello,²³ M. Dell'Orso,²³ L. Demortier,²⁷ B. Denby,²³ M. Deninno,² P. F. Derwent,¹⁷ T. Devlin,²⁸ J. R. Dittmann,⁶ S. Donati,²³ J. Done,³⁰ T. Dorigo,²¹ A. Dunn,¹⁷ N. Eddy,¹⁷ K. Einsweiler,¹⁵ J. E. Elias,⁷ R. Ely,¹⁵ E. Engels, Jr.,²⁴ D. Errede,¹¹ S. Errede,¹¹ Q. Fan,²⁶ I. Fiori,² B. Flaugher,⁷ G. W. Foster,⁷ M. Franklin,⁹ M. Frautschi,³¹ J. Freeman,⁷ J. Friedman,¹⁶ T. A. Fuess,¹ Y. Fukui,¹⁴ S. Funaki,³² G. Gagliardi,²³ S. Galeotti,²³ M. Gallinaro,²¹ M. Garcia-Sciveres,¹⁵ A. F. Garfinkel,²⁵ C. Gay,⁹ S. Geer,⁷ D. W. Gerdes,¹⁷ P. Giannetti,²³ N. Giokaris,²⁷ P. Giromini,⁸ L. Gladney,²² D. Glenzinski,¹³ M. Gold,¹⁹ J. Gonzalez,²² A. Gordon,⁹ A. T. Goshaw,⁶ K. Goulianatos,²⁷ H. Grassmann,²³ L. Groer,²⁸ C. Grossos-Pilcher,⁵ G. Guillian,¹⁷ R. S. Guo,²⁹ C. Haber,¹⁵ E. Hafner,¹⁶ S. R. Hahn,⁷ R. Hamilton,⁹ R. Handler,³⁴ R. M. Hans,³⁵ K. Hara,³² A. D. Hardman,²⁵ B. Harral,²² R. M. Harris,⁷ S. A. Hauger,⁶ J. Hauser,⁴ C. Hawk,²⁸ E. Hayashi,³² J. Heinrich,²² K. D. Hoffman,²⁵ M. Hohlmann,^{1,5} C. Holck,²² R. Hollebeek,²² L. Holloway,¹¹ A. Hölscher,¹² S. Hong,¹⁷ G. Houk,²² P. Hu,²⁴ B. T. Huffman,²⁴ R. Hughes,²⁶ J. Huston,¹⁸ J. Huth,⁹ J. Hylen,⁷ H. Ikeda,³² M. Incagli,²³ J. Incandela,⁷ G. Introzzi,²³ J. Iwai,³² Y. Iwata,¹⁰ H. Jensen,⁷ U. Joshi,⁷ R. W. Kadel,¹⁵ E. Kajfasz,^{7,*} T. Kamon,³⁰ T. Kaneko,³² K. Karr,³³ H. Kasha,³⁵ Y. Kato,²⁰ T. A. Keaffaber,²⁵ L. Keeble,⁸ K. Kelley,¹⁶ R. D. Kennedy,²⁸ R. Kephart,⁷ P. Kesten,¹⁵ D. Kestenbaum,⁹ R. M. Keup,¹¹ H. Keutelian,⁷ F. Keyvan,⁴ B. Kharadja,¹¹ B. J. Kim,²⁶ D. H. Kim,^{7,*} H. S. Kim,¹² S. B. Kim,¹⁷ S. H. Kim,³² Y. K. Kim,¹⁵ L. Kirsch,³ P. Koehn,²⁶ K. Kondo,³² J. Konigsberg,⁹ S. Kopp,⁵ K. Kordas,¹² W. Koska,⁷ E. Kovacs,^{7,*} W. Kowald,⁶ M. Krasberg,¹⁷ J. Kroll,⁷ M. Kruse,²⁵ T. Kuwabara,³² S. E. Kuhlmann,¹ E. Kuns,²⁸ A. T. Laasanen,²⁵ N. Labanca,²³ S. Lammel,⁷ J. I. Lamoureux,³ T. LeCompte,¹¹ S. Leone,²³ J. D. Lewis,⁷ P. Limon,⁷ M. Lindgren,⁴ T. M. Liss,¹¹ N. Lockyer,²² O. Long,²² C. Loomis,²⁸ M. Loretta,²¹ J. Lu,³⁰ D. Lucchesi,²³ P. Lukens,⁷ S. Lusin,³⁴ J. Lys,¹⁵ K. Maeshima,⁷ A. Maghakian,²⁷ P. Maksimovic,¹⁶ M. Mangano,²³ J. Mansour,¹⁸ M. Mariotti,²¹ J. P. Marriner,⁷ A. Martin,¹¹ J. A. J. Matthews,¹⁹ R. Mattingly,¹⁶ P. McIntyre,³⁰ P. Melese,²⁷ A. Menzione,²³ E. Meschi,²³ S. Metzler,²² C. Miao,¹⁷ G. Michail,⁹ R. Miller,¹⁸ H. Minato,³² S. Miscetti,⁸ M. Mishina,¹⁴ H. Mitsushio,³² T. Miyamoto,³² S. Miyashita,³² Y. Morita,¹⁴ J. Mueller,²⁴ A. Mukherjee,⁷ T. Muller,⁴ P. Murat,²³ H. Nakada,³² I. Nakano,³² C. Nelson,⁷ D. Neuberger,⁴ C. Newman-Holmes,⁷ M. Ninomiya,³² L. Nodulman,¹ S. H. Oh,⁶ K. E. Ohl,³⁵ T. Ohmoto,¹⁰ T. Ohsugi,¹⁰ R. Oishi,³² M. Okabe,³² T. Okusawa,²⁰ R. Oliver,²² J. Olsen,³⁴ C. Pagliarone,² R. Paoletti,²³ V. Papadimitriou,³¹ S. P. Pappas,³⁵ S. Park,⁷ A. Parri,⁸ J. Patrick,⁷ G. Paulette,²³ M. Paulini,¹⁵ A. Perazzo,²³ L. Pescara,²¹ M. D. Peters,¹⁵ T. J. Phillips,⁶ G. Piacentino,² M. Pillai,²⁶ K. T. Pitts,⁷ R. Plunkett,⁷ L. Pondrom,³⁴ J. Proudfoot,¹ F. Ptahos,⁹ G. Punzi,²⁴ K. Ragan,¹² A. Ribon,²¹ F. Rimondi,² L. Ristori,²³ W. J. Robertson,⁶ T. Rodrigo,^{7,*} S. Rolli,²³ J. Romano,⁵ L. Rosenson,¹⁶ R. Roser,¹¹ W. K. Sakamoto,²⁶ D. Saltzberg,⁵ A. Sansoni,⁸ L. Santi,²³ H. Sato,³² V. Scarpine,³⁰ P. Schlabach,⁹ E. E. Schmidt,⁷ M. P. Schmidt,³⁵ A. Scribano,²³ S. Segler,⁷ S. Seidel,¹⁹ Y. Seiya,³² G. Sganos,¹² A. Sgolachia,² M. D. Shapiro,¹⁵ N. M. Shaw,²⁵ Q. Shen,²⁵ P. F. Shepard,²⁴ M. Shimojima,³² M. Shochet,⁵ J. Siegrist,¹⁵ A. Sill,³¹ P. Sinervo,¹² P. Singh,²⁴ J. Skarha,¹³ K. Sliwa,³³ F. D. Snider,¹³ T. Song,¹⁷ J. Spalding,⁷ P. Sphicas,¹⁶ F. Spinella,²³ M. Spiropulu,⁹ L. Spiegel,⁷ L. Stancu,²¹ J. Steele,³⁴ A. Stefanini,²³ K. Strahl,¹² J. Strait,⁷ R. Ströhmer,⁹ D. Stuart,⁷ G. Sullivan,⁵ A. Soumarokov,²⁹ K. Sumorok,¹⁶ J. Suzuki,³² T. Takada,³² T. Takahashi,²⁰ T. Takano,³² K. Takikawa,³² N. Tamura,¹⁰ F. Tartarelli,²³ W. Taylor,¹² P. K. Teng,²⁹ Y. Teramoto,²⁰ S. Tether,¹⁶ D. Theriot,⁷ T. L. Thomas,¹⁹ R. Thun,¹⁷ M. Timko,³³ P. Tipton,²⁶ A. Titov,²⁷ S. Tkaczyk,⁷ D. Toback,⁵ K. Tollefson,²⁶ A. Tollestrup,⁷ J. Tonnison,²⁵ J. F. de Troconiz,⁹ S. Truitt,¹⁷ J. Tseng,¹³ N. Turini,²³ T. Uchida,³² N. Uemura,³² F. Ukegawa,²²

G. Unal,²² S. C. van den Brink,²⁴ S. Vejcik III,¹⁷ G. Velev,²³ R. Vidal,⁷ M. Vondracek,¹¹ D. Vucinic,¹⁶ R. G. Wagner,¹ R. L. Wagner,⁷ J. Wahl,⁵ C. Wang,⁶ C. H. Wang,²⁹ G. Wang,²³ J. Wang,⁵ M. J. Wang,²⁹ Q. F. Wang,²⁷ A. Warburton,¹² T. Watts,²⁸ R. Webb,³⁰ C. Wei,⁶ C. Wendt,³⁴ H. Wenzel,¹⁵ W. C. Wester III,⁷ A. B. Wicklund,¹ E. Wicklund,⁷ R. Wilkinson,²² H. H. Williams,²² P. Wilson,⁵ B. L. Winer,²⁶ D. Wolinski,¹⁷ J. Wolinski,¹⁸ X. Wu,²³ J. Wyss,²¹ A. Yagil,⁷ W. Yao,¹⁵ K. Yasuoka,³² Y. Ye,¹² G. P. Yeh,⁷ P. Yeh,²⁹ M. Yin,⁶ J. Yoh,⁷ C. Yosef,¹⁸ T. Yoshida,²⁰ D. Yovanovitch,⁷ I. Yu,³⁵ J. C. Yun,⁷ A. Zanetti,²³ F. Zetti,²³ L. Zhang,³⁴ W. Zhang,²² and S. Zucchelli²

(CDF Collaboration)

¹Argonne National Laboratory, Argonne, Illinois 60439

²Istituto Nazionale di Fisica Nucleare, University of Bologna, I-40126 Bologna, Italy

³Brandeis University, Waltham, Massachusetts 02254

⁴University of California at Los Angeles, Los Angeles, California 90024

⁵University of Chicago, Chicago, Illinois 60637

⁶Duke University, Durham, North Carolina 27708

⁷Fermi National Accelerator Laboratory, Batavia, Illinois 60510

⁸Laboratori Nazionali di Frascati, Istituto Nazionale di Fisica Nucleare, I-00044 Frascati, Italy

⁹Harvard University, Cambridge, Massachusetts 02138

¹⁰Hiroshima University, Higashi-Hiroshima 724, Japan

¹¹University of Illinois, Urbana, Illinois 61801

¹²Institute of Particle Physics, McGill University, Montreal, Canada H3A 2T8

and University of Toronto, Toronto, Canada M5S 1A7

¹³The Johns Hopkins University, Baltimore, Maryland 21218

¹⁴National Laboratory for High Energy Physics (KEK), Tsukuba, Ibaraki 305, Japan

¹⁵Lawrence Berkeley Laboratory, Berkeley, California 94720

¹⁶Massachusetts Institute of Technology, Cambridge, Massachusetts 02139

¹⁷University of Michigan, Ann Arbor, Michigan 48109

¹⁸Michigan State University, East Lansing, Michigan 48824

¹⁹University of New Mexico, Albuquerque, New Mexico 87131

²⁰Osaka City University, Osaka 588, Japan

²¹Università di Padova, Istituto Nazionale di Fisica Nucleare, Sezione di Padova, I-35131 Padova, Italy

²²University of Pennsylvania, Philadelphia, Pennsylvania 19104

²³Istituto Nazionale di Fisica Nucleare, University and Scuola Normale Superiore of Pisa, I-56100 Pisa, Italy

²⁴University of Pittsburgh, Pittsburgh, Pennsylvania 15260

²⁵Purdue University, West Lafayette, Indiana 47907

²⁶University of Rochester, Rochester, New York 14627

²⁷Rockefeller University, New York, New York 10021

²⁸Rutgers University, Piscataway, New Jersey 08854

²⁹Academia Sinica, Taipei, Taiwan 11529, Republic of China

³⁰Texas A&M University, College Station, Texas 77843

³¹Texas Tech University, Lubbock, Texas 79409

³²University of Tsukuba, Tsukuba, Ibaraki 305, Japan

³³Tufts University, Medford, Massachusetts 02155

³⁴University of Wisconsin, Madison, Wisconsin 53706

³⁵Yale University, New Haven, Connecticut 06511

(Received 20 February 1995)

The lifetimes of the B^- and \bar{B}^0 mesons are measured using the partially reconstructed semileptonic decays $\bar{B} \rightarrow D\ell^-\bar{\nu}\ell$, where D is either a D^0 or D^{*-} meson. The data were collected by the CDF detector at the Fermilab Tevatron collider during 1992–1993 and correspond to 19.3 pb^{-1} of $\bar{p}p$ collisions at $\sqrt{s} = 1.8 \text{ TeV}$. We measure the decay length distributions and find the lifetimes to be $\tau(B^-) = 1.56 \pm 0.13 \pm 0.06 \text{ ps}$ and $\tau(\bar{B}^0) = 1.54 \pm 0.08 \pm 0.06 \text{ ps}$, and the ratio of lifetimes to be $\tau(B^-)/\tau(\bar{B}^0) = 1.01 \pm 0.11 \pm 0.02$, where the first uncertainties are statistical and the second are systematic. [S0031-9007(96)00268-2]

PACS numbers: 13.20.He, 14.40.Nd

A measurement of the lifetimes of the different B -hadron species probes their decay mechanism beyond the simple spectator model decay picture. Possible causes of lifetime differences include the strength of the annihilation and the W -exchange graphs, and final state Pauli in-

terference effects. These mechanisms play an important role in the decay of charm hadrons; however, they are expected to produce smaller lifetime differences in the B hadrons, of order (5–10)% between B^- and \bar{B}^0 and 1% between \bar{B}^0 and \bar{B}_s^0 [1].

Several direct measurements of B^- and \bar{B}^0 meson lifetimes have been performed by the e^+e^- experiments and by CDF [2]. Indirect information has been obtained through the measurement of branching ratios [3,4]. The precision of current measurements now approaches the level where the predicted small differences could be discerned, and improvements in these measurements will provide a strong test of B -hadron decay mechanisms.

In this Letter we report a measurement of the B^- and \bar{B}^0 meson lifetimes using partially reconstructed semileptonic decays. The data used in this analysis were collected in 1992–93 with the CDF detector at the Fermilab Tevatron $\bar{p}p$ collider at a center-of-mass energy $\sqrt{s} = 1.8$ TeV, and correspond to an integrated luminosity of 19.3 pb^{-1} . Events with a lepton (e^- or μ^- , denoted by ℓ^-) associated with a D^0 or D^{*+} meson are selected. (Throughout this Letter a reference to a particular charge state also implies its charge conjugate). The ℓ^-D^{*+} candidates consist mostly of \bar{B}^0 decays, and the ℓ^-D^0 candidates consist mostly of B^- decays. The D^0 meson is reconstructed using the decay mode $D^0 \rightarrow K^-\pi^+$. The D^{*+} decays are reconstructed using the decay mode $D^{*+} \rightarrow D^0\pi^+$, followed by $D^0 \rightarrow K^-\pi^+$, $K^-\pi^+\pi^+\pi^-$, or $K^-\pi^+\pi^0$. The decay length distribution are measured and the lifetimes are extracted after correcting for the relative admixtures of B^- and \bar{B}^0 in the samples.

The CDF detector is described in detail elsewhere [5]. We describe here only the detector components most relevant to this analysis. Inside the 1.4 T solenoid the silicon vertex detector (SVX) and the central tracking chamber (CTC) provide the tracking and momentum analysis of charged particles. The CTC covers the pseudorapidity interval $|\eta| < 1.1$, where $\eta = -\ln[\tan(\theta/2)]$ [6]. The SVX gives a track impact parameter resolution of about $(13 + 40/p_T) \mu\text{m}$ [7], where p_T is the transverse momentum of the track in GeV/c . The transverse profile of the Tevatron beam is circular and has an rms spread of $\sim 35 \mu\text{m}$. Electromagnetic and hadronic calorimeters outside the solenoid cover the pseudorapidity region $|\eta| < 1.1$. Two muon subsystems are used, the central muon chambers and the central upgrade muon chambers.

Events containing semileptonic B decays are collected using inclusive lepton triggers. The $E_T (\equiv E \sin \theta)$ threshold for the principle single electron trigger is 9 GeV. The single muon trigger p_T threshold is 7.5 GeV/c . The specific criteria used for electron and muon identification are described in Refs. [8,9].

To identify the ℓ^-D^0 candidates, we search for $D^0 \rightarrow K^-\pi^+$ decays near the leptons, removing events that are consistent with the $D^{*+} \rightarrow D^0\pi^+$ decay chain. The $D^0 \rightarrow K^-\pi^+$ decay is reconstructed as follows. We first select oppositely charged pairs of particles using CTC tracks, where the kaon mass is assigned to the particle with the same charge as the lepton (called the “right sign” combination), as is the case in semileptonic

B decays. The kaon (pion) candidate is then required to have momentum above 1.5 (0.5) GeV/c , and to be within a cone of radius 0.6 (0.7) around the lepton in η - φ space. We require the decay vertex of the D^0 candidate to be positively displaced along its flight direction in the transverse plane with respect to the position of the primary vertex. The primary vertex is approximated by the beam position [9]. To remove events consistent with the decay chain $D^{*+} \rightarrow D^0\pi^+$, we combine additional positive tracks with the D^0 candidate and compute the mass difference (Δm) between the $D^0\pi^+$ and the D^0 , assigning the pion mass to the tracks; we remove events with Δm values between 0.142 and 0.148 GeV/c^2 . The resulting $K^-\pi^+$ invariant mass spectrum is shown in Fig. 1(a). We define the signal region to be in the mass range 1.84 to 1.88 GeV/c^2 . The total number of events in the signal region is 1233 with an estimated background fraction of 0.53 ± 0.03 . Also shown by the shaded histogram is the mass spectrum for the “wrong sign” ($K^+\pi^-$ with ℓ^-) combinations, where no significant signal is observed.

To identify ℓ^-D^{*+} candidates, we search for $D^{*+} \rightarrow D^0\pi^+$ decays using two fully reconstructed D^0 decay modes, $D^0 \rightarrow K^-\pi^+$ and $D^0 \rightarrow K^-\pi^+\pi^+\pi^-$, and one partially reconstructed mode, $D^0 \rightarrow K^-\pi^+\pi^0$. For the fully reconstructed modes, the D^0 candidate has to be in the mass ranges 1.83 to 1.90 GeV/c^2 and 1.84 to 1.88 GeV/c^2 , respectively. For the partially reconstructed mode, we require the mass of a $K^-\pi^+$ pair to

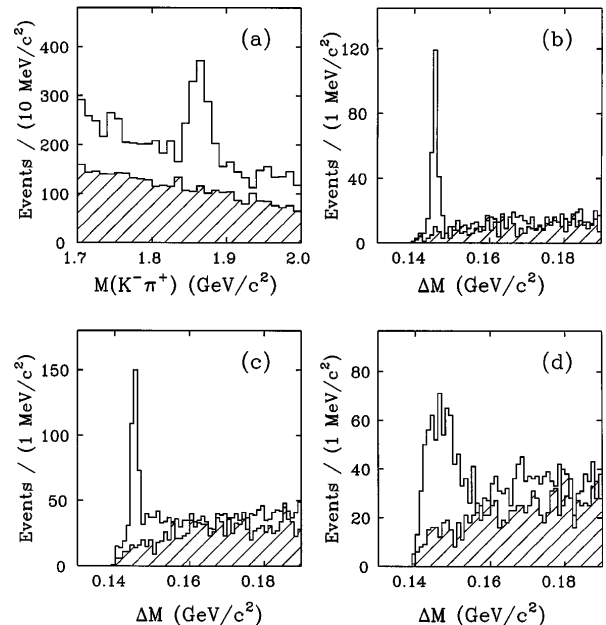


FIG. 1. Reconstructed charm signals in lepton events. Four modes are shown: (a) $D^0 \rightarrow K^-\pi^+$ (non D^{*+}), (b) $D^{*+} \rightarrow D^0\pi^+$, $D^0 \rightarrow K^-\pi^+$, (c) $D^{*+} \rightarrow D^0\pi^+$, $D^0 \rightarrow K^-\pi^+\pi^+\pi^-$, and (d) $D^{*+} \rightarrow D^0\pi^+$, $D^0 \rightarrow K^-\pi^+\pi^0$. Plot (a) shows the $K^-\pi^+$ invariant mass spectra, and (b)–(d) show the Δm distributions. Shaded histograms show wrong sign combinations, and in (a) they are scaled by 0.5 for display purposes.

be between 1.5 and 1.7 GeV/c^2 ; we do not reconstruct the π^0 and in the subsequent analysis treat the $K^-\pi^+$ pair as if it were a D^0 . We require positive decay lengths in the last two modes. For each mode, we reconstruct the D^{*+} meson by combining an additional track, assumed to have the pion mass, with the D^0 candidate, and computing the mass difference, Δm , between the $D^0\pi^+$ and D^0 . Figures 1(b)–1(d) show the Δm distributions, where the shaded histograms correspond to the wrong sign ($D^0\pi^-$) combinations. In Fig. 1(d) the peak is broadened because of the missing π^0 . We define the signal region as follows. The two fully reconstructed modes use the Δm range 0.144 to 0.147 GeV/c^2 , and the $K^-\pi^+\pi^0$ mode uses the range $\Delta m < 0.155 \text{ GeV}/c^2$. The numbers of events in the signal regions are 200, 332, and 704, with estimated background fractions of 0.11 ± 0.03 , 0.18 ± 0.03 , and 0.40 ± 0.03 , respectively.

The secondary vertex V_B is obtained by intersecting the trajectory of the lepton track with the flight path of the D^0 candidate. The B decay length L is defined as the displacement in the transverse plane of V_B from the primary vertex, projected onto the transverse momentum vector of the lepton- D^0 system. In semileptonic decays, the B meson momentum cannot be measured precisely because of the missing neutrino. We use the $p_T(\ell^-D^0)$ as an estimator of the B momentum, resulting in a corrected decay length $\xi = Lm(B)/p_T(\ell^-D^0)$ which we call the “pseudoproper decay length.” The distribution of the momentum ratio $\kappa = p_T(\ell^-D^0)/p_T(B)$ is obtained from a Monte Carlo calculation and is used in the subsequent lifetime fits. It has an average value of about 0.85 with an rms width of 0.11, and is approximately independent of the D^0 decay modes and of the $p_T(\ell^-D^0)$.

The lifetime is determined from a maximum likelihood fit to the observed pseudoproper decay length distributions. The signal probability function \mathcal{F}_{sig} consists of an exponential function $\exp(-\kappa\xi/c\tau)$ defined for positive decay lengths, convoluted with the κ distribution and a Gaussian distribution with width $s\sigma_i$. Here σ_i is the estimated resolution of ξ for event i , typically 100 μm , and the scale factor s accounts for a possible underestimate of the decay length resolution. The ξ distribution of combinatorial background events is described by a sum of a Gaussian distribution centered at zero, and positive and negative exponential tails. The shape of the background function and the scale factor s are determined from a simultaneous fit of a signal sample and a background sample. The background sample for the $D^0 \rightarrow K^-\pi^+$ mode is formed from the sidebands defined by the mass ranges 1.72 to 1.80 and 1.92 to 2.00 GeV/c^2 . For the D^{*+} modes, we use the right sign sideband, $0.15 < \Delta m < 0.19 \text{ GeV}/c^2$ for the two fully reconstructed modes, $0.16 < \Delta m < 0.19 \text{ GeV}/c^2$ for the $D^0 \rightarrow K^-\pi^+\pi^0$ mode, and the wrong sign sideband, $\Delta m < 0.19 \text{ GeV}/c^2$, for all three modes.

Figure 2 shows the ξ distributions of the events in the signal regions. Also shown by curves are the results of the

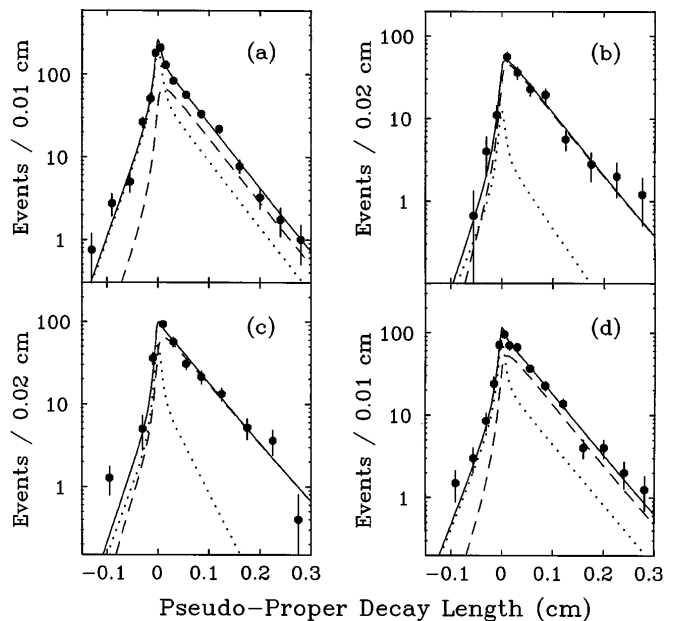


FIG. 2. Distributions of pseudoproper decay lengths for the lepton- D signal samples (points). Also shown are results of lifetime fits, signal (dashed curve) and background (dotted curve) contributions, and the sum of the two (solid curve). The four decay modes (a)–(d) are the same as in Fig. 1.

lifetime fit, with signal and background contributions. We find the lifetimes to be $c\tau(B) = 472 \pm 31$, 486 ± 42 , 497 ± 38 , and $451 \pm 31 \mu\text{m}$, where uncertainties are statistical only. As a check of the procedure, we measure the D^0 lifetime using the proper decay length measured from the secondary vertex V_B to the D decay vertex. The result, $133 \pm 12 \mu\text{m}$ averaged over the samples, is in reasonably good agreement with the world average value, $124.4 \pm 1.2 \mu\text{m}$ [10].

In order to extract the \bar{B}^0 and B^- lifetimes, we must take into account the fact that the ℓ^-D^0 and ℓ^-D^{*+} samples are admixtures of the neutral and charged B meson decays. The semileptonic decays can be expressed as $\bar{B} \rightarrow \ell^-\bar{\nu}\mathbf{D}$, where \mathbf{D} is a charm system whose charge is correlated with the B meson charge. If only the two lowest lying states, pseudoscalar (D) and vector (D^*), are produced, the ℓ^-D^{*+} combination can arise only from the \bar{B}^0 decay. Similarly the ℓ^-D^0 combination comes only from B^- decays, provided that the D^0 from the D^{*+} decay is excluded. However, higher mass D^{**} states (including nonresonant $D^{(*)}\pi$ pairs) are also produced in semileptonic B meson decays and their decays can dilute the charge correlation. Nevertheless, the ℓ^-D^0 and ℓ^-D^{*+} combinations are dominated by B^- and \bar{B}^0 meson decays, respectively.

We estimate the fraction g^- of the B^- decays in the ℓ^-D^0 and ℓ^-D^{*+} samples as follows. The production rates of charged and neutral B mesons and their semileptonic decay widths are assumed to be equal. We also assume the D^{**} decays exclusively to $D^{(*)}\pi$

via the strong interaction, thereby allowing us to determine the branching ratios, e.g., $D^{(*)+}\pi^0$ vs $D^{(*)0}\pi^+$, using isospin symmetry. We consider four factors affecting the composition. Firstly, the composition depends on the D^{**} fraction (f^{**}) in semileptonic B decays, which has been measured to be $f^{**} = 0.36 \pm 0.12$ [4]. Secondly, g^- depends on the relative abundance of four possible spin-parity D^{**} states, some of which decay only to $D^*\pi$ and others to $D\pi$. Changing the abundance is equivalent to changing the branching ratios for $D^*\pi$ and $D\pi$ averaged over various D^{**} states. We define a quantity $P_V = \mathcal{B}(D^{**} \rightarrow D^*\pi)/[\mathcal{B}(D^{**} \rightarrow D^*\pi) + \mathcal{B}(D^{**} \rightarrow D\pi)]$, where \mathcal{B} denotes a branching ratio. We assume the relative abundance found in Ref. [11] with $P_V = 0.78$. We also consider the extreme values $P_V = 0.0$ and 1.0 . Thirdly, the composition depends on the lifetime ratio, because the number of ℓ^-D events is proportional to the semileptonic branching ratio, which is the product of the lifetime and the partial width. Finally, the sample composition depends on the reconstruction efficiency of the low energy pion in the decay $D^{*+} \rightarrow D^0\pi^+$. If we miss the pion and reconstruct the D^0 , the D^{*+} is included in the ℓ^-D^0 sample and the sample composition is altered. The efficiency is measured to be $\epsilon(\pi) = 0.93^{+0.07}_{-0.21}$. We find that $g^- = 0.85^{+0.05}_{-0.12}$ for the ℓ^-D^0 sample and $g^- = 0.10^{+0.09}_{-0.10}$ for the ℓ^-D^{*+} sample when the two lifetimes are identical. The quoted uncertainties reflect maximum changes in g^- when f^{**} , P_V , and $\epsilon(\pi)$ are changed within quoted ranges. We have ignored small ($\sim 2\%$) contributions to the leptonic $D^{(*)}$ events from physics processes like $\bar{B}_s^0 \rightarrow \ell^-\bar{\nu}D_s^{*+}$, $D_s^{*+} \rightarrow D^{(*)}K$. Therefore the fraction of \bar{B}^0 mesons is given by $g^0 = 1 - g^-$.

We can now determine the B^- and \bar{B}^0 lifetimes with a combined fit of the ℓ^-D^0 and ℓ^-D^{*+} samples. We use a two-component signal distribution function given by $\mathcal{F}_{\text{sig}} = g^-\mathcal{F}_{\text{sig}}^- + (1 - g^-)\mathcal{F}_{\text{sig}}^0$, where $\mathcal{F}_{\text{sig}}^-$ and $\mathcal{F}_{\text{sig}}^0$ represent the charged and neutral B meson components, respectively. The dependence of g^- on the lifetime ratio is taken into account in the lifetime fits.

The sample composition is a source of systematic uncertainty in the B meson lifetime determination. We change the parameters f^{**} , P_V , and $\epsilon(\pi)$ within the quoted ranges, compute the sample composition g^- and fit the B meson lifetimes. We interpret the observed changes as systematic uncertainties; they are listed in Table I, together with other sources considered in this analysis. Alternative shapes for the background decay length distributions are considered and gives only minimal changes in the result. Physics backgrounds are studied by adding their simulated decay length distributions to the background function. Other sources of systematic uncertainties include our estimate of decay length resolution and of the B meson momentum. Also we have applied a loose decay length cut in some modes, and it introduces a slight bias in the lifetimes. Finally, a possible residual misalign-

TABLE I. A summary of systematic uncertainties in the B^- and \bar{B}^0 lifetime measurement.

Source	Contribution to		
	$c\tau(B^-)$ (μm)	$c\tau(\bar{B}^0)$ (μm)	$\frac{\tau(B^-)}{\tau(\bar{B}^0)}$
Sample composition	± 3	± 4	± 0.003
Background treatment	± 3	± 3	± 0.009
Decay length resolution	$+9$ -8	$+6$ -4	$+0.007$ -0.009
Momentum estimate	± 12	± 12	...
Decay length cut	$+0$ -5	$+0$ -5	± 0.016
Detector alignment	± 10	± 10	...
Beam stability	± 5	± 5	...
Total	± 19	± 18	$+0.020$ -0.021

ment of the SVX detector and the stability of the position of the Tevatron beam are considered. Some of these uncertainties cancel in the determination of the lifetime ratio. All these effects are combined in quadrature to give the total systematic uncertainty.

Our final result is $\tau(B^-) = 1.56 \pm 0.13 \pm 0.06 \text{ ps}$, $\tau(\bar{B}^0) = 1.54 \pm 0.08 \pm 0.06 \text{ ps}$, $\frac{\tau(B^-)}{\tau(\bar{B}^0)} = 1.01 \pm 0.11 \pm 0.02$ where the first uncertainties are statistical and the second are systematic. The result is consistent with other recent measurements [2]. At present, the two lifetimes are identical to each other within the uncertainty, consistent with the small difference predicted. They are also identical to the \bar{B}_s^0 lifetime [12] within the uncertainty.

We thank the Fermilab staff and the technical staffs of the participating institutions for their vital contributions. This work was supported by the U.S. Department of Energy and National Science Foundation; the Italian Istituto Nazionale di Fisica Nucleare; the Ministry of Education, Science and Culture of Japan; the Natural Sciences and Engineering Research Council of Canada; the National Science Council of the Republic of China; the A.P. Sloan Foundation; and the Alexander von Humboldt-Stiftung.

*Visitor.

- [1] M. B. Voloshin and M. A. Shifman, Sov. Phys. JETP **64**, 698 (1986); I. I. Bigi *et al.*, in *B Decays*, edited by S. Stone (World Scientific, Singapore, 1994), 2nd ed.; I. I. Bigi, Report No. UND-HEP-95-BIGO2, 1995.
- [2] F. Abe *et al.*, Phys. Rev. Lett. **72**, 3456 (1994); P. Abreu *et al.*, Z. Phys. C **57**, 181 (1993); P. Abreu *et al.*, Phys. Lett. B **312**, 253 (1993); D. Buskulic *et al.*, Phys. Lett. B **307**, 194 (1993); **325**, 537(E) (1994); R. Akers *et al.*, Z. Phys. C **67**, 379 (1995); D. Buskulic *et al.*, Report No. CERN-PPE/96-14, 1996 (to be published).
- [3] M. Athanas *et al.*, Phys. Rev. Lett. **73**, 3503 (1994); **74**, 3090(E) (1995); H. Albrecht *et al.*, Phys. Lett. B **275**, 195 (1992); H. Albrecht *et al.*, Z. Phys. C **54**, 1 (1992); H. Albrecht *et al.*, Phys. Lett. B **232**, 554 (1989).

- [4] R. Fulton *et al.*, Phys. Rev. D **43**, 651 (1991).
- [5] F. Abe *et al.*, Nucl. Instrum. Methods Phys. Res., Sect. A **271**, 387 (1988), and references therein.
- [6] In CDF, φ is the azimuthal angle, θ is the polar angle measured from the proton direction, and r is the radius from the beam axis (z axis).
- [7] D. Amidei *et al.*, Nucl. Instrum. Methods Phys. Res., Sect. A **350**, 73 (1994).
- [8] F. Abe *et al.*, Phys. Rev. Lett. **71**, 500 (1993).
- [9] F. Abe *et al.*, Phys. Rev. Lett. **71**, 3421 (1993).
- [10] Particle Data Group, L. Montanet *et al.*, Phys. Rev. D **50**, 1173 (1994).
- [11] N. Isgur, D. Scora, B. Grinstein, and M. Wise, Phys. Rev. D **39**, 799 (1989).
- [12] F. Abe *et al.*, Phys. Rev. Lett. **74**, 4988 (1995); P. Abreu *et al.*, Z. Phys. C **61**, 407 (1994); D. Buskulic *et al.*, Phys. Lett. B **322**, 275 (1994); R. Akers *et al.*, Phys. Lett. B **350**, 273 (1995).